

**You might find this additional information useful...**

---

This article cites 53 articles, 24 of which you can access free at:

<http://jn.physiology.org/cgi/content/full/78/5/2693#BIBL>

This article has been cited by 11 other HighWire hosted articles, the first 5 are:

**Subthreshold Sodium Current Underlies Essential Functional Specializations at Primary Auditory Afferents**

S. Curti, L. Gomez, R. Budelli and A. E. Pereda  
*J Neurophysiol*, April 1, 2008; 99 (4): 1683-1699.  
[\[Abstract\]](#) [\[Full Text\]](#) [\[PDF\]](#)

**Contribution of NMDA and AMPA Receptors to Temporal Patterning of Auditory Responses in the Inferior Colliculus**

J. T. Sanchez, D. Gans and J. J. Wenstrup  
*J. Neurosci.*, February 21, 2007; 27 (8): 1954-1963.  
[\[Abstract\]](#) [\[Full Text\]](#) [\[PDF\]](#)

**Representation of Auditory Signals in the M-Cell: Role of Electrical Synapses**

T. M. Szabo, S. A. Weiss, D. S. Faber and T. Preuss  
*J Neurophysiol*, April 1, 2006; 95 (4): 2617-2629.  
[\[Abstract\]](#) [\[Full Text\]](#) [\[PDF\]](#)

**Connexin35 Mediates Electrical Transmission at Mixed Synapses on Mauthner Cells**

A. Pereda, J. O'Brien, J. I. Nagy, F. Bukauskas, K. G. V. Davidson, N. Kamasawa, T. Yasumura and J. E. Rash  
*J. Neurosci.*, August 20, 2003; 23 (20): 7489-7503.  
[\[Abstract\]](#) [\[Full Text\]](#) [\[PDF\]](#)

**Chemical synaptic activity modulates nearby electrical synapses**

M. Smith and A. E. Pereda  
*PNAS*, April 15, 2003; 100 (8): 4849-4854.  
[\[Abstract\]](#) [\[Full Text\]](#) [\[PDF\]](#)

Medline items on this article's topics can be found at <http://highwire.stanford.edu/lists/artbytopic.dtl> on the following topics:

Physiology .. Synaptic Transmission  
Cell Biology .. Glutamate Receptors  
Oncology .. N-Methyl-D-Aspartate Receptors  
Biochemistry .. Aspartate  
Neuroscience .. Glutamate  
Oncology .. Synaptic Potentials

Updated information and services including high-resolution figures, can be found at:

<http://jn.physiology.org/cgi/content/full/78/5/2693>

Additional material and information about *Journal of Neurophysiology* can be found at:

<http://www.the-aps.org/publications/jn>

---

This information is current as of February 10, 2010 .

# A Fast Synaptic Potential Mediated by NMDA and Non-NMDA Receptors

LAURA R. WOLSZON, ALBERTO E. PEREDA, AND DONALD S. FABER

*Department of Neurobiology and Anatomy, MCP ♦ Hahnemann School of Medicine, Allegheny University of the Health Sciences, Philadelphia, Pennsylvania 19129*

**Wolszon, Laura R., Alberto E. Pereda, and Donald S. Faber.** A fast synaptic potential mediated by NMDA and non-NMDA receptors. *J. Neurophysiol.* 78: 2693–2706, 1997. Excitatory synaptic transmission in the CNS often is mediated by two kinetically distinct glutamate receptor subtypes that frequently are colocalized, the *N*-methyl-D-aspartate (NMDA) and non-NMDA receptors. Their synaptic currents are typically very slow and very fast, respectively. We examined the pharmacological and physiological properties of chemical excitatory transmission at the mixed electrical and chemical synapses between auditory afferents and the goldfish Mauthner cell, *in vivo*. Previous physiological data have suggested the involvement of glutamate receptors in this fast excitatory postsynaptic potential (EPSP), the chemical component of which decays with a time constant of <2 ms. We demonstrate here that the pharmacological and voltage-dependent characteristics of the synaptic currents are consistent with glutamatergic transmission and that both NMDA and non-NMDA receptors are involved. The two components surprisingly exhibit quite similar kinetics even at resting potential, with the NMDA response being only slightly slower. Due to its fast kinetics and characteristic voltage dependence, NMDA receptor-mediated transmission at these first-order synapses contributes significantly to paired pulse and frequency-dependent facilitation of successive fast EPSPs during high-frequency repetitive firing, a presynaptic impulse pattern that induces activity-dependent homosynaptic changes in both electrical and chemical transmission. Thus NMDA receptor kinetics in this intact preparation are suited to its functional requirements, namely speed of information transmission and the ability to trigger changes in synaptic efficacy.

## INTRODUCTION

Presynaptic release of glutamate mediates excitatory neurotransmission at most central vertebrate synapses, via interactions at the postsynaptic membrane with two classes of ligand-gated ion channels, *N*-methyl-D-aspartate (NMDA) and non-NMDA [ $\alpha$ -amino-3-hydroxy-5-methyl-4-isoxazolepropionic acid (AMPA)], receptors (McBain and Mayer 1994). These two channel types usually are colocalized and contribute kinetically distinct components to the excitatory postsynaptic currents (EPSCs) shaping fast synaptic transmission. Whereas the conductance changes mediated by AMPA receptor channels usually have a fast onset and rapid decay, those due to NMDA receptors are typically long lasting, having a slower rate of rise and a prolonged deactivation (Jahr 1994; McBain and Mayer 1994).

The kinetics of NMDA receptor-mediated excitatory postsynaptic potentials (EPSPs) depend on both channel properties and the degree of voltage-dependent block by  $Mg^{2+}$ , which is nearly complete at resting potential (Nowak et al.

1984). Thus the EPSP decay depends enormously on whether the membrane remains sufficiently depolarized to depress the  $Mg^{2+}$  block. In fact, fast NMDA receptor-mediated EPSPs have been observed in hippocampus after single stimuli (Thomson and Radpour 1990). On the other hand, it generally is assumed that repeated synaptic stimulation provides the ideal “priming” depolarization, allowing the expression of these synaptic currents (Herron et al. 1986; Jahr 1994; McBain and Mayer 1994). It therefore has been speculated that NMDA receptors confer Hebbian properties to glutamatergic synapses, such that they respond to presynaptically released glutamate only when there is sufficient postsynaptic depolarization. The resultant  $Ca^{2+}$  influx then can induce activity-dependent changes in synaptic strength, such as long- and short-term potentiation and depression (see Malenka and Nicoll 1993).

Synaptic plasticity also occurs at the junctions between auditory afferents and the Mauthner (M) cell in the goldfish, where a wealth of evidence shows that transmission at these terminals can be modified by homosynaptic input activity (Pereda and Faber 1996; Yang and Faber 1991; Yang et al. 1990). The parent axons of these afferents, which originate in the sacculus, send one branch each to the distal part of the M cell lateral dendrite where they terminate as single, large, myelinated club endings (LMCEs) (Bartelmez 1915), each having both chemical synapses and gap junctional plaques (Nakajima and Kohno 1978; Tuttle et al. 1986). Thus electrical stimulation of the posterior eighth nerve produces a biphasic excitatory response consisting of a fast electrotonic component, or coupling potential, followed by a chemically mediated EPSP with a time constant of decay of <2 ms (Furshpan 1964; Lin and Faber 1988a). The EPSP waveform reflects the kinetics of the activated synaptic channels because the M cell’s membrane time constant is  $\sim 400 \mu s$  (Fukami et al. 1964). This speed of transmission, which is a requirement for the initiation of the sound-evoked escape response mediated via the M cell and its output circuitry (Faber et al. 1989), would make it unlikely that NMDA-receptor activation underlies activity-dependent plasticity of these junctions. However, previous results suggested that the chemical EPSP may be mediated by glutamate (Diamond 1968; Titmus et al. 1996; Wolszon and Faber 1988). Moreover, long-term potentiation (LTP) of both components of the mixed synaptic response produced by posterior eighth nerve tetanization is prevented by NMDA receptor antagonists and by postsynaptic injections of the  $Ca^{2+}$  chelator bis-(*o*-aminophenoxy)-*N,N,N',N'*-tetraacetic acid (Pereda and

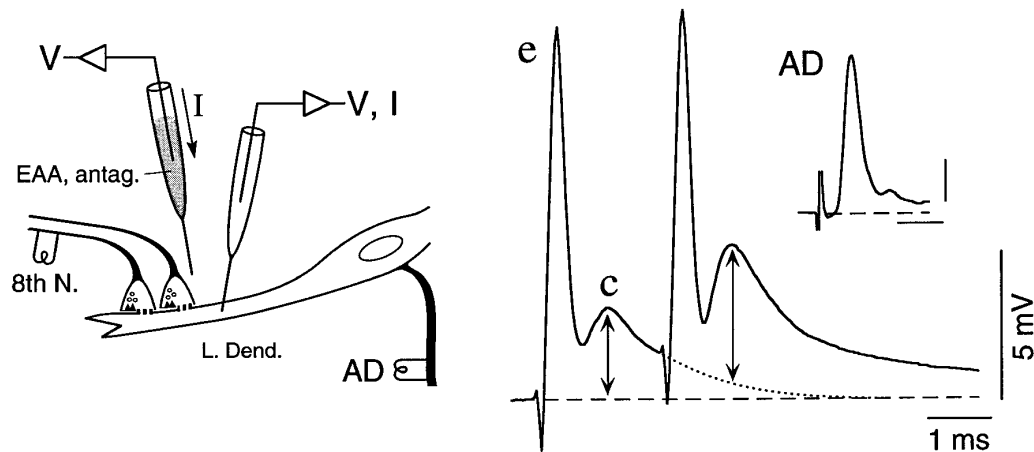


FIG. 1. Recording arrangement and characteristic responses to orthodromic and antidromic Mauthner (M)-cell activation. *Left*: schematic representation of the right M-cell, viewed dorsally, with anterior toward the *top*. Voltage ( $V$ ) and current ( $I$ ) recordings were made from the lateral dendrite (L. Dend.) during orthodromic (8th N) or antidromic (AD) stimulation. Excitatory amino acids (EAA) and antagonists (antag.) were pressure-ejected outside the region where the 8th-N fibers contact the M-cell dendrite, or dissolved in saline and superfused over the brain. *Right*: stimulating the eighth nerve while recording from the M cell lateral dendrite produces a 2-component excitatory postsynaptic potential (EPSP): a rapid electrical potential ( $e$ ) followed by a chemical potential ( $c$ ; amplitude indicated by first  $\leftrightarrow$ ). Responses to double stimuli illustrate the enhancement of the second chemical EPSP (second  $\leftrightarrow$ ) due to paired-pulse facilitation. Second EPSP amplitude typically was measured using the tail of a single response as the baseline ( $\cdots$ , extrapolated decay of the first EPSP). *Inset*: typical antidromic action potential. Amplitude of this spike, which, because of the electrical inexcitability of the M-cell soma and dendrites, propagates only passively along the lateral dendrite, is a reliable measure of changes in the input resistance of the M cell (Faber and Korn 1978). All traces are the average of  $\geq 10$  sweeps;  $- - -$  (here and in subsequent figures), baseline continuations. Calibration bars in the *inset* are also 5 mV and 1 ms.

Faber 1996; Yang et al. 1990). Finally, recent immunohistochemical evidence demonstrates that both NMDA and non-NMDA receptors are found in the distal part of the M cell lateral dendrite (Sur et al. 1994) where these afferents terminate (Lin et al. 1983).

We present here pharmacological and physiological evidence supporting the notions that the neurotransmitter at the LMCE is indeed glutamate and that it acts by activating both NMDA and non-NMDA postsynaptic receptors. Strikingly, the 2-amino-5-phosphonovaleric acid (APV)-sensitive (NMDA) component is present at the relatively high resting potential of the M cell ( $-80$  mV), and its kinetics are much faster than those previously reported in other systems (McBain and Mayer 1994) despite the lower temperature of this preparation. These differences suggest that the goldfish NMDA-receptor proteins operate under different physiological conditions in this intact preparation and also may be unusual in sequence or subunit combination. Further, the kinetic properties of the NMDA receptor-mediated responses are shown to be responsible for a frequency-dependent facilitation of the chemical EPSP, a critical requirement for the induction of activity-dependent changes in its synaptic strength.

## METHODS

### General electrophysiological techniques

Goldfish 10–12 cm in length were anesthetized with MS-222 (Ethyl m-aminobenzoate; 250 mg/l) and then paralyzed with D-tubocurarine hydrochloride ( $3 \mu\text{g/g}$  body weight). The preparation and general electrophysiological techniques were similar to those previously described (Faber and Korn 1978; Furshpan and Furu-

kawa 1962; Korn and Faber 1975a; Lin and Faber 1988a). Briefly, the skull was removed, the brain and eighth nerve exposed, and intracellular recordings then performed *in vivo* from the medullary region. The M cell was penetrated with microelectrodes filled with either 2.5 M KCl or 5 M K acetate (Ac). Electrode resistances ranged from 3 to 20 M $\Omega$ . A bipolar stimulating electrode was placed on the spinal cord near the tail to antidromically activate the M cell, generating extracellular field potentials that assist in the cell's localization (Furshpan and Furukawa 1962). For orthodromic activation via the eighth nerve, a 10- to 20-M $\Omega$  microstimulating bipolar electrode (Longreach Scientific Resources, Orr's Island, ME), with tip diameters of  $\sim 10 \mu\text{m}$ , was placed on the nerve,  $\sim 800 \mu\text{m}$  outside the brain (Lin 1986; Lin and Faber 1988a). This stimulating electrode was insulated except at the very tips, which were offset relative to each other and separated by  $\sim 100 \mu\text{m}$  to permit fine control of stimulus location and strength. All experiments were performed at room temperature ( $\sim 22^\circ\text{C}$ ).

### Extracellular pressure-ejection of excitatory amino acid antagonists

The recording electrodes for these experiments contained 5 M KAc (with resistances of 10–16 M $\Omega$ ), and the M cell lateral dendrite was impaled 200–250  $\mu\text{m}$  from the cell body, a locus including the region where the eighth nerve fibers contact the M cell (Fig. 1). The drug electrodes contained either  $\gamma$ -D-glutamylglycine (DGG) or DL-APV (100 mM, pH 8.0) in 2 M NaCl and had resistances of 8–18 M $\Omega$ . They were placed 250  $\mu\text{m}$  from the M cell soma, their tips being between 10 and 100  $\mu\text{m}$  dorsal to its lateral dendrite. Control intracellular records were taken after the M-cell penetration had stabilized, as indicated by the constancy of the neuron's antidromic spike, resting membrane potential, and responses to eighth nerve inputs. Drugs then were applied in the form of continuous pressure pulses of 5–15 psi, during which time the responses of the M cell to eighth nerve and antidromic

stimulation (0.4–5 Hz) were monitored. When the drugs were observed to have achieved their maximum effects at a given pressure, the pressure was released, but the position of the electrode maintained, and the recoveries of M-cell responses recorded. Resting potentials ranged from  $-81$  to  $-89$  mV and were very stable throughout the experiments, as were the amplitudes of the antidromic spikes. Given the distance between the pressure electrode and the M cell, volume dilution, and difficulties inherent to extracellular pressure injection, we estimate the effective concentrations of the drugs were at least two orders of magnitude less than in the pipette. However, to guarantee specificity, they also were applied by superfusion over a wide range of concentrations.

### Superfusion of antagonists

Recording electrodes for the superfusion experiments had resistances of 7–11 M $\Omega$  and impaled the dendrite 175–275  $\mu$ m distal to the M cell soma. For this experimental series, the goldfish brain was superfused continuously with normal fish saline [containing (in mM) 124 NaCl, 5.1 KCl, 3.0 NaH<sub>2</sub>PO<sub>4</sub>·H<sub>2</sub>O, 0.9 MgSO<sub>4</sub>·7H<sub>2</sub>O, 1.6 CaCl<sub>2</sub>·2H<sub>2</sub>O, 5.6 glucose, and 20.0 *N*-2-hydroxyethylpiperazine-*N'*-2-ethanesulfonic acid, pH 7.2), either with or without the addition of 6-cyano-7-nitroquinoxaline-2,3-dione (CNQX; 50  $\mu$ M), DL-APV (5–150  $\mu$ M), ketamine (20–50  $\mu$ M), or a mixture of APV and ( $\pm$ )-3-(2-carboxypiperazin-4-yl)-propyl-1-phosphonic acid (CPP; 50  $\mu$ M each). During initial cell localization, and while taking control (pre-drug) records of eighth nerve M-cell responses, drug-free saline was superfused and then drug was added while maintaining the electrode penetration by switching the solution to one containing the drug dissolved in saline. The new fluid was delivered at a nearly identical rate, and the level of solution over the brain ( $\approx$ 0.5 ml) remained constant. However, to rule out the possibility that very small changes in fluid flow might alter the recording or stimulation conditions, in some experiments ( $n = 7$ ), we first monitored responses while changing from one solution of saline to another and then subsequently switched to the drug-containing solution.

Because the dead volume in the superfusion apparatus was  $\sim$ 0.2 ml and the flow rate was 5–10 ml/min, the time before the start of the solution change ranged from 20 to 40 s. However, because the M cell lies 1.5 mm below the surface of the medulla but is close to the surface of the fourth ventricle, the time for the actual diffusion of the drug into or out of the synaptic regions of interest cannot be gauged accurately. Based on the time courses of the effects, diffusion was sometimes complete within as little as 5 min, although in other instances the drug actions were fully manifest only after 1 h.

When possible, drug was applied until the magnitude of its effects stabilized; the values reported here were measured at those plateaus. The superfusion solution then was changed back to drug-free saline. This wash-out often took much longer than the time required for the effect of the drug to be manifest; therefore, it was usually difficult or impossible to maintain a stable electrode penetration until there was a complete reversal of drug effects.

To ensure that any effects on eighth nerve EPSP amplitudes were not due to changes in M-cell input resistance, the antidromic spike height was monitored throughout these experiments, as the soma-dendritic membranes are electrically inexcitable (see Faber and Korn 1978).

### General voltage-clamp techniques

The discontinuous single-electrode voltage-clamp (SEVC) technique (Axoclamp 2, Axon Instruments) was used to record synaptic or agonist-induced currents while controlling M cell membrane potential. Two-electrode voltage clamp could not be employed because dual dendritic penetrations with large electrode tips were

difficult to maintain. Sampling rates varied between 16 and 25 kHz; the signals were filtered at 10 kHz. Recording electrodes (containing 2.5 M KCl or 5 M KAc) had resistances between 2.5 and 5 M $\Omega$ . For experiments in which synaptic currents were examined, only KAc electrodes were used to avoid possible chloride-loading of the M cell. The recording electrodes impaled the M cell lateral dendrite 150–250  $\mu$ m from the soma.

As the space constant of the dendrite is approximately 250  $\mu$ m (Faber and Korn 1978), we assume that in the best conditions the voltage in the region of the dendrite that receives input from the LMCEs was probably well clamped. It was usually difficult to clamp the dendrite to levels very far beyond the resting potential because of the low input resistance of the M cell ( $\sim$ 150 k $\Omega$  in the soma and from 400 k $\Omega$  to 2 M $\Omega$  in the dendrite) and occasional instabilities of electrode resistance. Great care was taken, therefore, to ensure that excitatory currents were stable and reproducible, and any measurements obtained under unstable conditions were omitted from the subsequent analyses. For this reason, the current-voltage data were acquired over limited voltage ranges; in one experiment, the electrode maintained a stable clamp for potential changes as great as  $\pm$ 35 mV from rest, but it was more common to be limited to  $\pm$ 10–20 mV.

### Tests for voltage-dependence of glutamatergic responses and synaptic currents

To test the voltage dependence of M-cell responses to glutamate agonists, we applied continuous depolarizing or hyperpolarizing voltage steps. Once a stable membrane current was obtained, pressure pulses of glutamate or NMDA (1 M, pH 7.2) were ejected from a second (extracellular) electrode and the M-cell responses were recorded. The order in which the voltage was clamped to different values was randomized, and each step usually was repeated a number of times to test for reproducibility of response amplitudes. In the case of the eighth nerve EPSCs, steps of 10- to 25-ms duration were applied with and without superimposed eighth nerve EPSCs. Synaptic currents were measured by subtracting the leak currents produced by the same voltage steps without concurrent nerve stimulation.

Because of the short latency and rapid rise of the eighth nerve electrotonic potential, the voltage-clamp apparatus could not control membrane potential quickly enough to reliably record this current.

### Data analysis

Data were digitized (7–12  $\mu$ s sampling interval) and averaged on-line with a DEC LSI/11–73 computer connected to an INDEC data-acquisition system or with a Macintosh-based system. They also were recorded on tape or VCR (5–10 kHz cutoff frequency) for subsequent, more detailed analysis.

Exponential fits of the time courses of decay of eighth nerve EPSCs were achieved using a nonlinear least-squares algorithm with uniform weighting of the data points after compensation for baseline offsets (BINFITS, courtesy of Dr. Christopher Lingle, Washington University, St. Louis). Data points were chosen for inclusion in the fits by visual estimation of the 20–80% amplitude range of the largest response; then all responses from a particular experiment were fit within the same time frame. The error limits are expressed as 90% confidence limits; these were usually small, a typical value for the time constant of decay being  $1.38 \pm 0.019$  ms (mean  $\pm$  SD).

## RESULTS

The recording arrangement and general experimental paradigm are illustrated schematically in Fig. 1, *left*, and typical

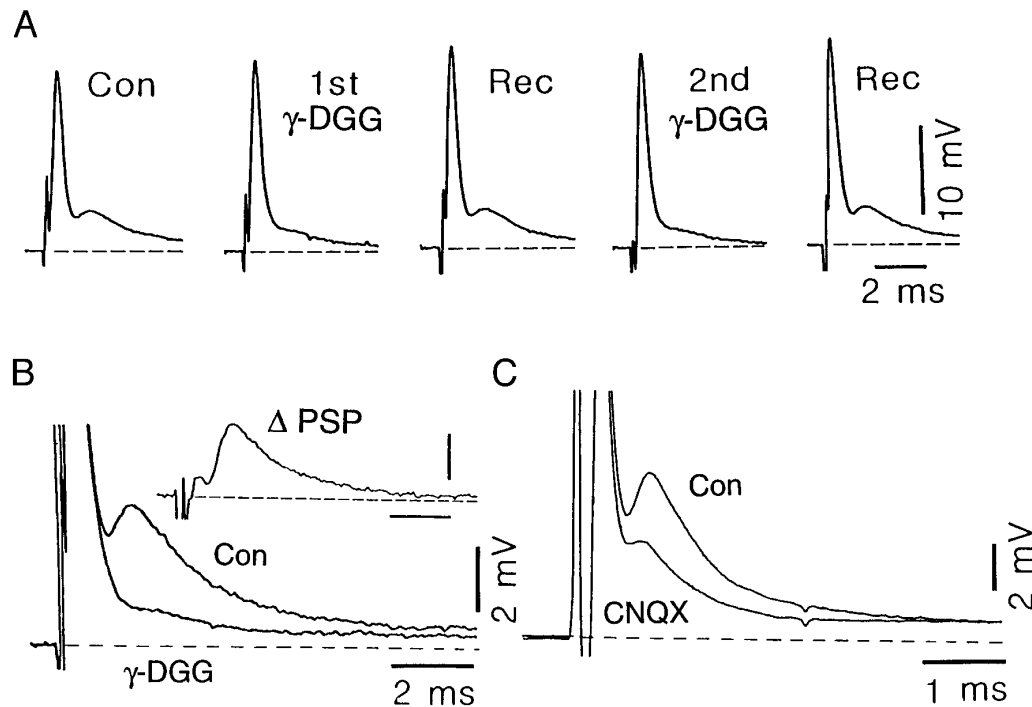


FIG. 2. Chemical EPSP is antagonized by  $\gamma$ -D-glutamylglycine (DGG) and 6-cyano-7-nitroquinoxaline-2,3-dione (CNQX). *A* and *B*: to determine if the chemical EPSP is mediated by an excitatory amino acid, 100 mM  $\gamma$ -DGG, a nonselective excitatory amino acid antagonist, was pressure-applied to the region of the eighth nerve synaptic input. *A*: successive applications (1st  $\gamma$ -DGG, 2nd  $\gamma$ -DGG) reversibly abolished the EPSP (Con, control; Rec, recovery). *B*: superposition of a control and a postdrug EPSP from the same experiment, at higher application pressure (15 psi). *Inset*: digital subtraction of control and test responses, revealing the amplitude and waveform of the  $\gamma$ -DGG-sensitive component ( $\Delta$ PSP). Electrical component (off-scale) was unaffected. Traces are averages of 5 sweeps. *C*: superimposed high gain recordings obtained in the control and 20 min after beginning superfusion with the non-NMDA receptor antagonist CNQX (50  $\mu$ M), confirming a partial block of the chemical EPSP. As in *B*, the coupling potential is truncated.

intradendritic responses to ortho- and antidromic stimulation in Fig 1, *right*. Given their characteristic large diameter (5–15  $\mu$ m) and consequent low-threshold LMCEs can be activated selectively by using weak stimuli to the posterior eighth nerve. The bimodal, monosynaptic PSPs (Furshpan 1964), evoked by paired-pulse stimulation of the eighth nerve in this example, consist of a rapid electrotonic coupling potential (Fig. 1, *e*) arising from current flow through gap junctions followed by a slower and smaller chemical EPSP (Fig. 1, *c*). Because of the short time constant of the M-cell membrane ( $\sim 400 \mu$ s) (Fukami et al. 1964), these components are distinguished easily, and their time courses largely represent those of the underlying currents (Faber and Korn 1978). The response amplitudes and waveforms are quite stable for  $\geq 2$  h during maintained intracellular recordings, as described previously (Pereda and Faber 1996; Pereda et al. 1992, 1994; Silva et al. 1995; Yang and Faber 1991; Yang et al. 1990). As shown in Fig. 1, the chemical EPSP is facilitated by the pairing of the stimuli, whereas electrical coupling is not. Figure 1, *inset*, shows the antidromic action potential, which is conducted passively along the soma and dendrite (see Faber and Korn 1978) and therefore reveals changes in M-cell input resistance. Although the amplitude of the first EPSP is measured with respect to baseline, there actually is a residual contribution from the coupling potential. Therefore, the percent reduction in EPSP size after drug application is slightly underestimated.

#### *Is the transmitter at the LMCE an excitatory amino acid?*

As mentioned above, although the identity of the neurotransmitter at these synapses was previously unknown, there is pharmacological (Diamond and Roper 1973; Faber and Korn 1978; Titmus et al. 1996; Wolszon and Faber 1988) and immunocytochemical (Sur et al. 1994) evidence for glutamate receptors on the lateral dendrite. In addition, NMDA receptor antagonists block the induction of activity-dependent LTP at these junctions (Pereda and Faber 1996; Yang et al. 1990). Therefore, we first asked whether the transmitter might be an excitatory amino acid by testing the effects of a nonspecific glutamate antagonist,  $\gamma$ -DGG (100 mM) (Jones et al. 1984) on the posterior eighth nerve-evoked EPSP ( $n = 3$ ). Extracellular pressure pulses were used using to apply the drug.

When  $\gamma$ -DGG was applied to the distal lateral dendrite, the chemical EPSP was diminished consistently, without any significant changes in the coupling potential or in the antidromic spike. Figure 2, *A* and *B*, illustrates this effect. Figure 2*A* contains the averaged M-cell responses recorded before and after two successive applications of the antagonist at 5 psi. The first application substantially reduced the EPSP within 60 s, without affecting the coupling potential, and recovery was complete within 4 min. The second drug application had the same reversible effect. To more fully illustrate the magnitude of  $\gamma$ -DGG antagonism of the chemical EPSP,

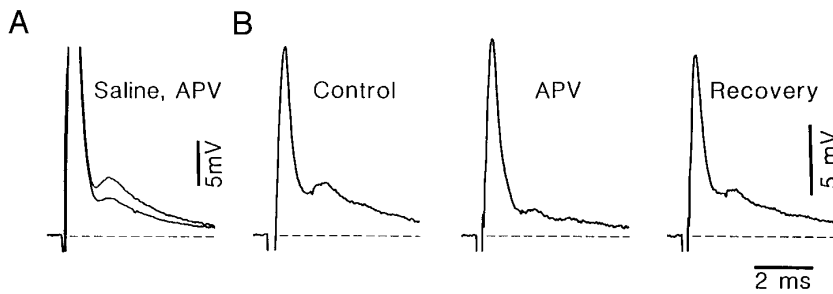


FIG. 3. Chemical EPSP is antagonized partially by pressure-application of 100 mM 2-amino-5-phosphonovaleric acid (APV), a selective *N*-methyl-D-aspartate (NMDA)-receptor antagonist. *A*: DL-APV (40 mM) reduced the chemical EPSP, but not the electrical, to 62% of its original amplitude. Pre- and postapplication EPSPs are superimposed, the coupling potentials being off-scale in this illustration. *B*: in another experiment, the control EPSP was reduced 50% within 10 min by DL-APV (100 mM) and then recovered to 89% of its original amplitude 12 min later. Note that the EPSPs are not as smooth here because of the relatively proximal (125  $\mu$ m lateral to the axon cap) recording site. Traces are averages of 8 sweeps.

a control and another test response are superimposed in Fig. 2*B*, at a higher gain than in *A*. In this case, a larger dose of  $\gamma$ -DGG was used (15 psi). The residual, slowly decaying tail after the rapid coupling potential resembles that seen with high-frequency eighth nerve stimulation (not shown: see Fig. 1 in Yang et al. 1990), which virtually eliminates the chemical component; therefore, the block was essentially complete. The tail is most likely a continuation of the rapid coupling potential, which has a small slow decay component. Figure 2*B*, *inset*, contains the difference between the two responses and reveals the waveform of the  $\gamma$ -DGG-sensitive component, the decay of which is similar to that of the control. The difference waveform also provides a clear representation of the EPSP's rising phase, uncontaminated by the electrical potential.

The chemical EPSPs were reduced to between 25 and 54% of their control amplitudes in this preliminary series of experiments. These effects were completely reversible in two of three experiments, with the amplitudes recovering to 102 and 106% of pre-ejection values. There was no change in either the antidromic spike amplitude or the membrane resting potential, indicating that the observed effects were not due to changes in input resistance. These data confirmed that the neurotransmitter at these synapses between the eighth nerve is an excitatory amino acid.

#### Are both non-NMDA and NMDA receptors involved?

It recently was shown that the chemical EPSP is blocked completely by pressure applications of a combination of APV and CNQX (Titmus et al. 1996), which together antagonize both NMDA and non-NMDA receptor-mediated responses, respectively. To determine whether both receptor subtypes are indeed involved, we studied the effects of individual antagonists on the eighth-nerve-evoked response.

We found that CNQX, an AMPA (or non-NMDA)-receptor antagonist, suppressed the chemical EPSP when applied by superfusion. Figure 2*C* illustrates an example in which this blocker (50  $\mu$ M) eliminated most, but not all, of the chemical component, providing further support for the involvement of glutamatergic transmission. However, DL-APV (pressure-injected, 100 mM), a NMDA-receptor-specific antagonist (Davies et al. 1981), also partially reduced the size of the chemical EPSPs, to within 50–68% of the control (pre-ejection) amplitudes (Fig. 3. *A* and *B*;  $n = 3$  of 4). These EPSPs subsequently recovered to between 89 and 95% of controls. Two of these experiments are illustrated in Fig. 3. Antidromic spike heights again were unaffected by the drug applications, and resting potentials changed by

only 2–3 mV. The fourth pressure injection experiment, using 20 mM APV, produced no effect (not shown). It is unlikely that the CNQX acted by blocking NMDA receptors at the glycine binding site (Birch et al. 1988; Hablitz and Sutor 1990; Yamada et al. 1988), as evidence that glycine iontophoresis has no effect on the EPSP suggests that the concentration of this amino acid is sufficiently high in vivo to saturate the receptor (D. S. Faber and M. J. Titmus, unpublished observations).

Very high concentrations of APV can antagonize non-NMDA receptors (reviewed in Mayer and Westbrook 1987; Stone and Burton 1988). Because it is impossible to know the actual drug concentration near the M-cell membrane when using extracellular pressure-ejection, we performed the same tests superfusing the brain, in vivo, with low doses of DL-APV, CPP, or ketamine, another specific NMDA antagonist (MacDonald et al. 1987). The appropriate doses for distinguishing between NMDA- and non-NMDA-mediated responses vary between systems, but a conservative estimate of the maximum allowable drug concentration for NMDA receptor selectivity is 50  $\mu$ M for ketamine and 50–100  $\mu$ M for DL-APV and CPP. Figure 4 demonstrates that superfusion with a mixture of DL-APV and CPP (50  $\mu$ M each) had the same effect as observed with pressure ejection. Specifically, the peak amplitude of the chemical EPSP was attenuated and the remaining response decayed slightly faster (Fig. 4, *A* and *C*). The small reduction in the coupling potential in the illustrated experiment was not a constant finding and might reflect a 5–7% decrease in input resistance. The effect on the chemical EPSP was appreciably greater, and, as shown (Fig. 4*B*), it persisted for the duration of the experiment. Finally, the difference waveform or APV/ CPP-sensitive component has a time course that is comparable to that of the control EPSP (Fig. 4*D*).

Because it was clear that the APV-sensitive component was not remarkably slower than the non-NMDA component (compare Figs. 2*C*, 3*A*, and 4*C*), as initially expected, we systematically quantified the EPSP reduction and the underlying kinetics, as schematized in Fig. 5*A*. For this purpose, the peak times of the pre- and postdrug EPSPs were indicated by  $t_1$  and  $t_2$ , respectively, and that of the drug-sensitive component ( $\Delta$ EPSP) by  $t_3$ . Because the chemical EPSP onset could be obscured by the coupling potential that preceded it, all peak times were referenced to the stimulus artifact. The percent reduction of the EPSP then was calculated at  $t_3$  and is given by:

$$\% \text{ Reduction} = (\Delta \text{EPSP}_{t_3} / \text{EPSP}_{\text{control}, t_3}) \times 100. \quad (1)$$

We found that both NMDA antagonists produced dose-

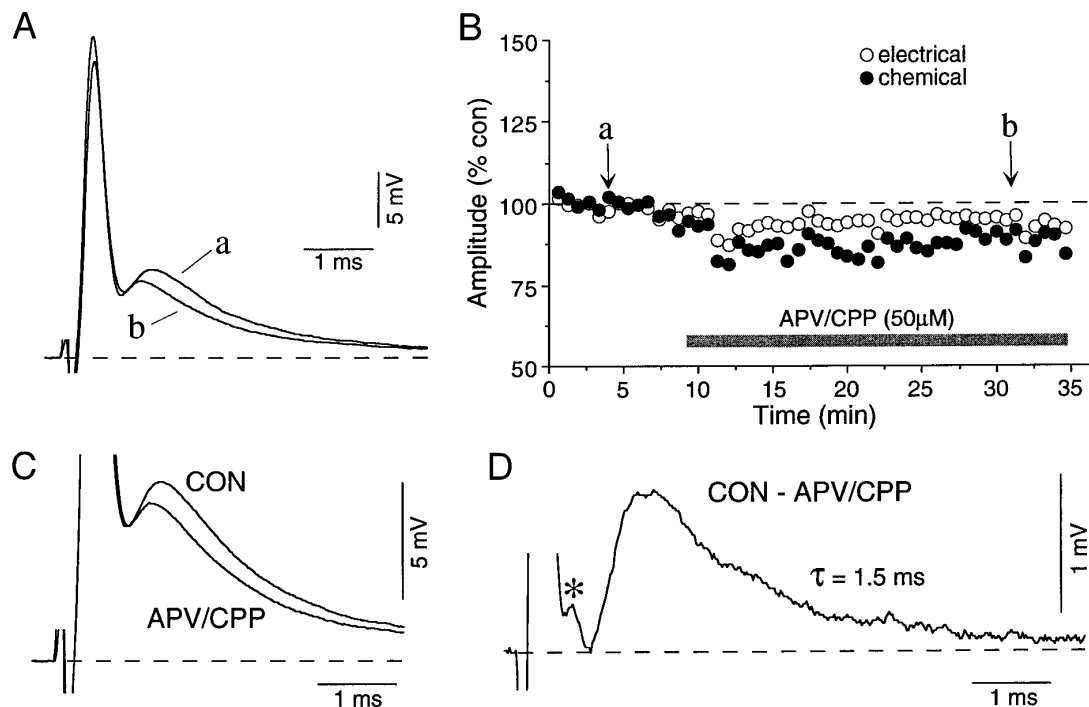


FIG. 4. Time course of the APV/CPP antagonism of 1 component of the chemical EPSP. *A–D*: effects of superfusion with  $50 \mu\text{M}$  each of APV and CPP. *A*: superimposed traces representing averages of 20 individual responses obtained before (*a*) and after (*b*) drug application. APV/CPP removes a small slightly delayed component of the synaptic response. *B*: time course of the normalized amplitudes of the electrical and chemical components of the synaptic response in control situation and after addition of APV/CPP to the superfusate. There was a permanent reduction in the chemical EPSP, whereas a slight decrease in the electrical component, not observed consistently, most likely represents an unspecific effect of the drug on M-cell input resistance. Each point represents the average of 20 individual responses. *C*: superimposed average traces ( $n > 200$ ) at high gain, from the control (CON) and during the last 7.5 min of the data plotted in *B*. *D*: computer-calculated difference between the waveforms displayed in *C*, representing the time course of the APV/CPP-sensitive component. Subtraction also showed the slight reduction in the electrical component (\*), which can be taken as an indicator of the timing of the presynaptic spike. Note the fast kinetics of the APV/CPP-sensitive component.

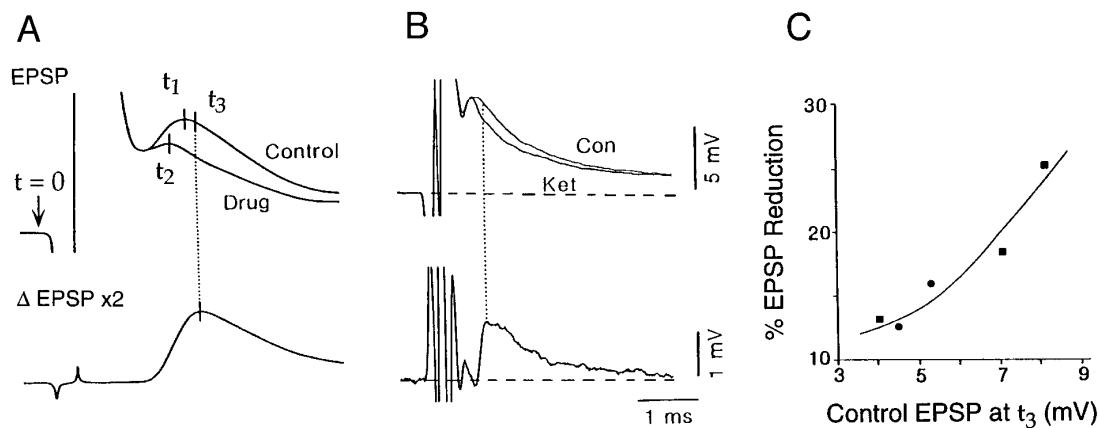


FIG. 5. Quantification of the antagonist effects. *A*, *top*: schematic diagram of 2 superimposed eighth nerve-evoked EPSPs, before (control) and after drug treatment. *Bottom*: illustration of how the subtracted PSP, now at twice the gain, typically appears. Amplitudes of the EPSPs were measured at 3 times:  $t_1$  defines the peak of the control PSP,  $t_2$  defines that of the drug-insensitive component, and  $t_3$  is the time at which the drug-sensitive component peaks. Percent reduction of the control EPSP was measured at  $t_3$  (···). Zero reference point for the time measurements was taken in the flat region of the baseline, just before the stimulus artifact. *B*: chemical EPSP is shown before (Con, Control) and 29 min after (Ket, ketamine) superfusion of the brain with  $50 \mu\text{M}$  ketamine in saline. Electrotonic potential was unaffected by the drug and therefore is truncated here. PSP produced after ketamine treatment was subtracted digitally from the control and is shown at higher gain (*bottom*). ···, drug-sensitive component peaks later than the control. Artifacts in the baseline preceding this component are due to the subtraction process and are magnified by the rapidity of the electrotonic potential. Traces are averages of 20–25 sweeps. *C*: percent reduction of the EPSP by ketamine is dependent on predrug EPSP amplitude. Magnitude of the percent reduction is plotted as a function of the original PSP amplitude for the 4  $50\text{-}\mu\text{M}$  ketamine experiments listed in Table 1. ●, values for 2 different stimulus strengths tested in 1 experiment (denoted by \* in Table 1). Curve fit by eye.

TABLE 1. Summary of ketamine and APV experiments

	Control EPSP			$\Delta$ EPSP		Residual EPSP			
	Peak, mv	$t_p (=t_1)$ , ms	Amplitude at $t_3$ , mv	Peak, mV	$t_p (=t_3)$ , ms	$t_p (=t_2)$ , ms	Percent reduction at $t_3$	Time, min	Recovery (to %)
Ketamine									
20 $\mu$ M	12.10	1.33	8.81	0.86	1.88	1.27	9.8	15	NA
50 $\mu$ M	8.97	1.22	8.16	2.05	1.38	1.10	25.1	52	85
50 $\mu$ M	4.79	1.01	4.04	0.53	1.24	0.98	13.1	19	NA
50 $\mu$ M	7.42	1.01	7.09	1.30	1.12	0.90	18.3	29	99
50 $\mu$ M, A*	4.66	0.98	4.49	0.57	1.09	0.94	12.7	5	NA
50 $\mu$ M, B*	5.28	0.92	5.29	0.84	0.94	0.89	15.9	5	NA
Mean, 50 $\mu$ M (using B, $n = 4$ )†	6.66 $\pm$ 0.97	1.04 $\pm$ 0.06	6.15 $\pm$ 0.92	1.18 $\pm$ 0.33	1.17 $\pm$ 0.09	0.97 $\pm$ 0.05	18.1 $\pm$ 2.6	—	—
APV									
5 $\mu$ M	5.54	0.98	5.53	0.97	1.18	0.98	17.9	51	NA
20 $\mu$ M	6.43	1.29	5.73	1.44	1.54	1.10	25.1	7	NA
20 $\mu$ M	5.06	0.97	4.38	0.38	1.22	0.97	8.7	18	106
50 $\mu$ M	5.18	1.10	5.01	0.61	1.28	1.01	12.1	5	NA
50 $\mu$ M†	5.68	1.36	5.54	1.77	1.49	1.22	32.0	22	NA
150 $\mu$ M†	5.68	1.36	5.60	2.51	1.46	1.02	44.8	27	66
100 $\mu$ M	6.31	1.34	6.08	1.79	1.54	1.41	29.4	31	77
100 $\mu$ M	6.21	1.52	6.18	1.27	1.55	1.53	20.6	21	NA
Mean, all ( $n = 8$ )†	5.77 $\pm$ 0.21	1.24 $\pm$ 0.07	5.51 $\pm$ 0.21	1.34 $\pm$ 0.25	1.41 $\pm$ 0.05	1.15 $\pm$ 0.08	23.8 $\pm$ 4.1	—	—

Values are means  $\pm$  SE. Definitions of peak times are illustrated in Fig. 5.  $\Delta$ EPSP (excitatory postsynaptic potential) is the subtracted drug-sensitive component; time column represents the time to reach steady state effect (see METHODS). APV 2-amino-5-phosphonovaleric acid;  $t_p$ , peak time; NA, not available (experiment terminated before significant recovery could be attained). \* In one experiment, the responses to two different stimulus strengths (A and B) were tested. † Two doses were tested in the same experiment.

dependent reductions in chemical EPSP amplitude. In the example of Fig. 5B, pre- and postketamine responses are superimposed (*top*) at a gain that truncates the coupling potentials. It is clear that the ketamine-insensitive EPSP reaches a peak earlier and decays faster: the EPSP amplitude was reduced by 18.3% at  $t_3$  and the drug-sensitive component removed a relatively late component (*bottom trace*) that peaked  $\sim 110 \mu$ s after that of the control. This result is typical of those found in five experiments with ketamine (20–50  $\mu$ M) and in seven with APV (5–100  $\mu$ M). In none of these experiments were the electrotonic PSP, antidromic spike height, or resting membrane potential affected by the antagonists.

Table 1 summarizes the results of all of the ketamine and DL-APV superfusion experiments. It should be stressed that although control peak times are in the range of 0.92 to 1.52 ms, these values are artificially large because we measured peak times from the beginning of the stimulus artifact. Had we been able to accurately distinguish the true EPSP onset (see Figs. 4D and 5B), actual peak times would be  $< 0.5$  ms. Note that one ketamine experiment examined drug effects at two different eighth nerve stimulus strengths (Table 1, \*), to determine whether different control EPSP amplitudes were differentially sensitive to the drug. This was found to be the case and is supported by data described below. In addition, when two concentrations of APV (50 and 150  $\mu$ M) were tested in the same experiment (Table 1, †), the larger dose had the greater effect.

We emphasize that quantitative comparison of drug effects between experiments, even using the same dose, is limited by two factors. First, in some experiments, it was not known whether the effects had reached a plateau, as the electrode penetration could not be maintained long enough.

This limitation also usually prevented testing for reversibility. Second, the diffusion time of the drug to the afferent synapses, which are 1.5 mm below the brain's surface (but within a few hundred micrometers of the ventricle), varied between preparations, possibly because of tissue differences. Therefore, absolute values for the percent reduction cannot necessarily be compared between experiments at a given time point. Nevertheless, in the 50  $\mu$ M ketamine experiments ( $n = 4$ ), the average percent reduction was relatively large, being  $18.1 \pm 2.6\%$  (mean  $\pm$  SE), compared with  $1.6 \pm 2.1\%$  in the controls ( $n = 7$ , saline to saline). Membrane potential was stable throughout these experiments, depolarizing by only  $2.2 \pm 2.0$  mV from beginning to end. Similarly, APV was found to reduce the EPSP by  $24.8 \pm 4.3\%$  ( $n = 8$ ; Table 1); the average reduction for doses of 50  $\mu$ M APV was 22.0%. Membrane potential depolarized by only  $0.8 \pm 1.8$  mV.

#### Effects of NMDA receptor antagonists on EPSP time course

Both ketamine and APV tended to decrease the peak times of the EPSPs, although these differences did not reach statistical significance. In the four 50- $\mu$ M ketamine experiments, the  $t_p$  of the control EPSP was  $1.04 \pm 0.06$  ms, whereas that of the remaining EPSP was  $0.97 \pm 0.05$  ms; the  $t_p$  of the ketamine-sensitive component was  $1.17 \pm 0.09$  ms. Similarly, in the APV experiments, the  $t_p$  of the EPSP decreased from  $1.24 \pm 0.07$  ms to  $1.15 \pm 0.08$  ms. The  $t_p$  of the APV-sensitive component ( $1.41 \pm 0.05$  ms), however, was significantly longer than that of the control.

When the ketamine and APV experiments are considered together, the peak time of the drug-sensitive component

( $t_3$ ) was always longer (Fig. 5A) than that of the residual EPSP ( $t_2$ ), the difference being  $>150 \mu\text{s}$  in 11 of 14 cases ( $256 \pm 42.2 \mu\text{s}$ ). When results obtained with the two antagonists were treated separately, the mean value of  $t_3$  was significantly longer than that of  $t_2$  ( $1.17 \pm 0.09 \text{ ms}$  vs.  $0.97 \pm 0.05 \text{ ms}$  for ketamine experiments,  $P < 0.05$ ;  $1.41 \pm 0.05 \text{ ms}$  vs.  $1.15 \pm 0.08 \text{ ms}$  for APV,  $P < 0.02$ ; Wilcoxon signed-rank test). Thus although it is not possible to measure accurately the onsets of the two components because of the electrical EPSP, the one putatively mediated by activation of NMDA receptors reaches its peak amplitude slightly later than the peak of the non-NMDA EPSP. Nevertheless, these differences are small, the major finding being that the two components are fast. Inspection of the  $\Delta\text{PSP}$  records suggests that the rise times (10–90% peak amplitude) of both are in the range of  $\leq 0.5$ .

To determine whether the durations of the NMDA and non-NMDA components differ, we performed exponential fits of the decays of the control and residual EPSPs (fits of  $\Delta\text{PSP}$ s were not achieved reliably). All but one of these waveforms were best fit by a single exponential. The time constants of decay for 11 of the control EPSPs (from 12 preparations) listed in Table 1 were  $1.17 \pm 0.09 \text{ ms}$  and  $0.93 \pm 0.07$  for the APV and ketamine experiments, respectively. Those for the residual drug-insensitive waveforms in the same experiments were  $1.25 \pm 0.12$  and  $0.90 \pm 0.07 \text{ ms}$ . Thus in each set of experiments, the two means were statistically indistinguishable ( $P > 0.1$ , Wilcoxon signed-rank test), indicating that the durations of the NMDA and non-NMDA components are equivalent at resting potential.

#### Dependence of the percent reduction on control EPSP amplitude

NMDA-mediated responses are enhanced by depolarizations that alleviate the  $\text{Mg}^{2+}$  block of the channel. Consequently, one might anticipate that the APV- or ketamine-sensitive component would contribute more to large control EPSPs than to small ones. In confirmation, we found a positive correlation between the control EPSP amplitude and the magnitude of the ketamine-induced reduction. This phenomenon is illustrated in Fig. 5C, in which the percent reduction, measured at the  $t_p$  of the ketamine-sensitive component ( $t_3$ ), is plotted as a function of the control EPSP amplitude. We did not attempt to make the same comparison for the APV experiments since widely varying drug concentrations were used.

The above correlation suggests that the NMDA-mediated component confers voltage dependence to the synaptic response. We therefore tested this possibility directly under voltage-clamp conditions.

#### Voltage dependence of synaptic currents

If part of a neuron's response to synaptic activation is mediated by NMDA receptors, depolarization beyond the resting potential should enhance that component by relieving a voltage-sensitive magnesium block (Mayer and Westbrook 1984; Mayer et al. 1984; Nowak et al. 1984). This phenomenon accounts for the region of negative-slope conductance near the resting potential during NMDA-mediated

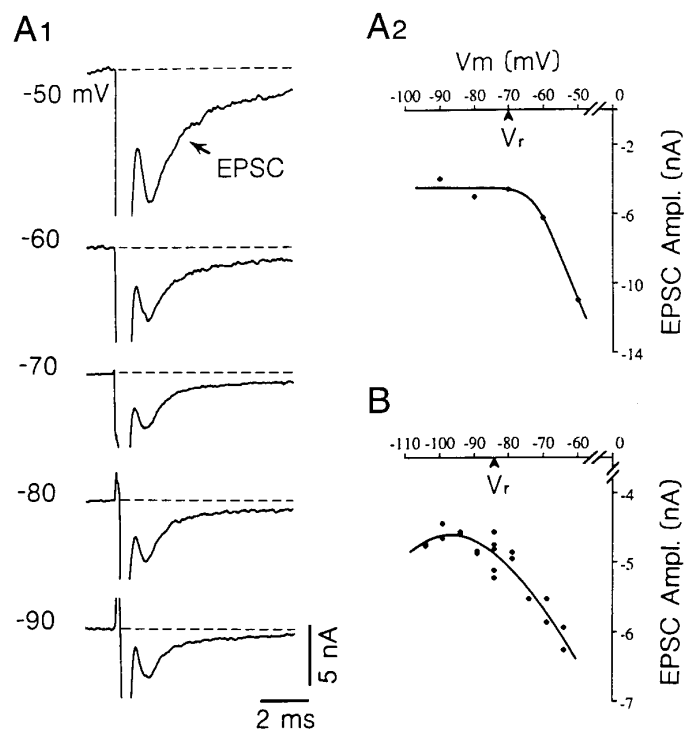


FIG. 6. Excitatory postsynaptic current (EPSC) arising from 8th-N stimulation is voltage dependent. *A1*: chemically mediated EPSC ( $\rightarrow$ ) was larger and possessed a different time course of decay at voltages more depolarized than the resting potential ( $V_r = -70 \text{ mV}$ ). Traces are the averages of 20–25 sweeps and are leak-subtracted. *I-V* curve for this experiment is shown in *A2*. *B*: similar data from another experiment. Curves fit by eye.

synaptic responses. To determine whether the excitatory responses recorded in the M cell exhibit this type of current-voltage relationship, we voltage-clamped the distal lateral dendrite while stimulating the posterior eighth nerve. These experiments were conducted with the SEVC technique (see METHODS).

The EPSCs studied in seven cells all exhibited a region of negative-slope conductance near the resting potential (from  $-70$  to  $-90 \text{ mV}$  in these experiments), suggestive of a synaptic response that at least partly is mediated by NMDA receptors. Two examples of such an experiment are shown in Fig. 6. Figure 6*A1* illustrates the voltage dependence of the leak-subtracted, averaged synaptic currents evoked by stimulating the eighth nerve. Depolarization of the cell to only 10 mV beyond rest (to  $-60 \text{ mV}$ ) caused a substantial enhancement of the EPSC; this enhancement was even more pronounced at  $-50 \text{ mV}$ . The current-voltage relationship for this experiment is shown in Fig. 6*A2*. Note the hyperpolarization beyond the resting potential did not significantly affect the synaptic current, suggesting that non-NMDA receptor-mediated conductances play a larger role in this voltage range. Depolarization beyond  $-50 \text{ mV}$  resulted in an unstable clamp condition, as discussed above, so it was impossible to determine whether the slope of the *I-V* curve would have reversed polarity had more positive membrane potentials been used.

The *I-V* curve in Fig. 6*B*, from a different experiment, illustrates another example of the negative-slope conductance. Although depolarization to  $-64 \text{ mV}$  was insufficient

to cause a reversal of the slope, it became slightly positive when the cell was hyperpolarized to between  $-94$  and  $-104$  mV, as would be expected if non-NMDA-mediated conductances dominated the curve in this region. We observed this phenomenon in six of seven experiments.

Because the voltage dependence of NMDA-mediated responses is due to magnesium block of the associated channel (Mayer et al. 1984; Nowak et al. 1984), we tested whether the current-voltage relationship of the EPSCs could be altered by perfusion with magnesium-free saline. After 40 min of superfusion, no effect was observed (not shown). This result is probably due to the difficulty of significantly reducing the magnesium concentration in an *in vivo* preparation, particularly when the synapses of interest are not at the surface of the brain and when magnesium-block can occur with even  $5 \mu\text{M}$  extracellular magnesium (Nowak et al. 1984).

#### Voltage dependence of EPSC kinetics

One would expect relatively complicated kinetics of EPSCs produced at mixed NMDA and non-NMDA synapses. We therefore tested whether single- and double-exponential functions fit the EPSC decays produced at various membrane potentials. Generally, a single exponential was sufficient to accurately describe the decays of the EPSCs and of the EPSPs (the latter being reliable indicators of the time course of conductance changes because the membrane time constant is  $\sim 0.5$  ms). When EPSC decays were fit with a double exponential, the fast component had a time constant similar to that obtained with a single exponential ( $\sim 1$  ms), whereas that of the smaller slow component varied with membrane potential, from  $\sim 2$  ms at  $-90$  mV to  $\sim 17$  ms at  $-50$  mV. In fact, the time constants of decay always tended to increase with depolarization, regardless of their single- or double-exponential origins.

#### Membrane responses to glutamate and NMDA applications

Although responses in the lateral dendrite to glutamate have been described previously (Diamond and Roper 1973), sensitivity to directly applied NMDA has not been demonstrated. We therefore tested whether functional NMDA receptors exist on the dendrite by applying it directly in voltage-clamp experiments and by asking whether the EPSC  $I$ - $V$  relations could be mimicked by NMDA or the putative transmitter glutamate. First M-cell responses to extracellular pressure-application of  $1 \text{ M}$  glutamate ( $n = 2$ ) were monitored. Amplitudes and durations of the pressure pulses were chosen to give reproducible responses without mechanically disturbing the dendritic membrane; a  $10$ -psi pulse for  $80$  ms was sufficient to elicit reproducible responses of comparable amplitudes. As shown in Fig. 7A, 1 and 2, there was a striking voltage dependence of the M cell's response to pressure-applied glutamate. Depolarization by even  $5$  mV from rest ( $-78$  to  $-73$  mV) substantially enhanced the amplitude of the current, whereas depolarization by  $10$  mV (to  $-68$  mV) more than tripled it. Conversely, hyperpolarization significantly reduced the glutamate response. The  $I$ - $V$  curve for this experiment is illustrated in Fig. 7A2. The steep negative

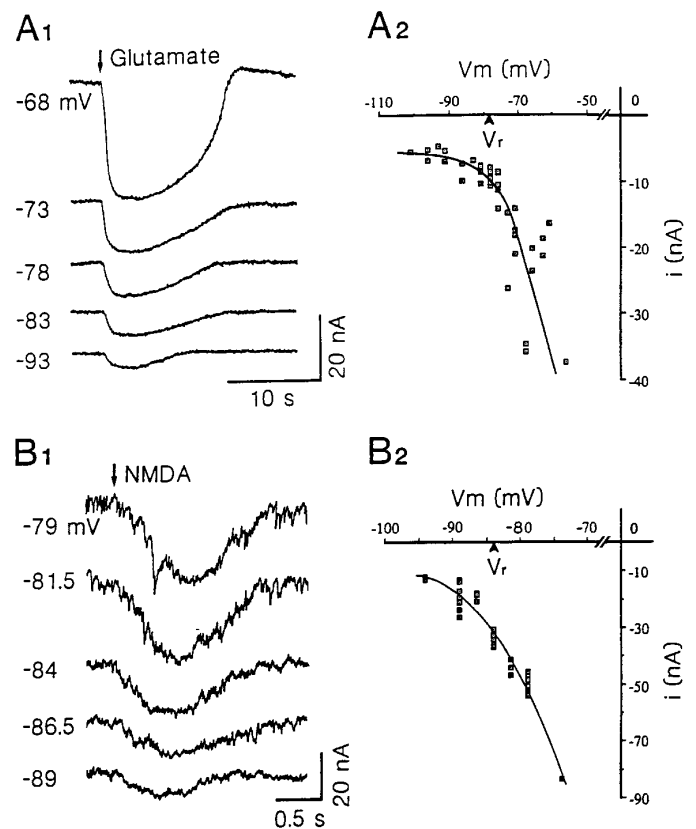


FIG. 7. Voltage dependence of M-cell responses to pressure-applied excitatory amino acids. *A*, 1 and 2: pressure pulses of glutamate ( $1 \text{ M}$ ) were applied outside the distal lateral dendrite while voltage-clamping this region of the cell. *A1*: M-cell responses to glutamate at the indicated holding potentials. Resting potential  $-78$  mV. Note that when the cell was depolarized by even  $5$  or  $10$  mV, the responses (inward currents) were enhanced dramatically. *A2*: corresponding  $I$ - $V$  curve for this experiment.  $V_r$ : resting potential. Curve fit by eye. *B*, 1 and 2: similar properties of responses to pressure-applied NMDA. *B1*: postsynaptic currents were enhanced markedly with even small levels of depolarization (resting potential =  $-84$  mV); in this case, a  $2.5$ -mV depolarization actually doubled the response. Brief inward current superimposed on the  $-79$  mV response is probably a spontaneous synaptic current. *B2*:  $I$ - $V$  curve for this experiment also has a region of negative-slope conductance near the resting potential ( $V_r$ ). Curve fit by eye.

slope of the curve can be seen in the region of the resting potential, but the slope approaches zero as the cell was hyperpolarized beyond  $-91$  mV. Hyperpolarization by even  $24$  mV beyond rest never caused the slope of the curve to become more positive. Similar results were found in the second experiment where, in addition, the slope conductance became positive as the cell was hyperpolarized by  $5$  mV (not shown).

We next tested directly whether there are NMDA receptors on the lateral dendrite, as suggested above and implied by immunocytochemical data (Sur et al. 1994). For this purpose, NMDA ( $1 \text{ M}$ ) was applied by pressure-ejection ( $n = 4$ ) using pulses of  $10$  to  $40$  psi and  $250$  to  $1,000$  ms duration. In every experiment, we found robust NMDA responses that were voltage sensitive, with regions of very steep negative-slope conductance near the resting potentials (which ranged from  $-63$  to  $-84$  mV). In the example of Fig. 7B, 1 and 2, it is remarkable that depolarization of only

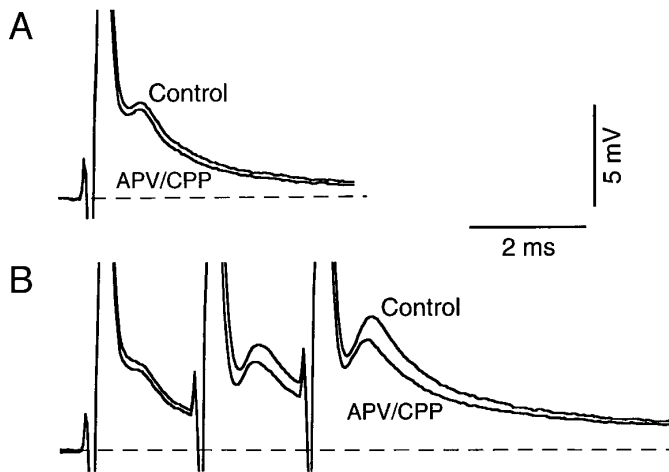


FIG. 8. Blocking effect of NMDA antagonists is progressively greater for successive EPSPs in a burst. Superimposed averaged records ( $n \geq 15$ ) obtained in control and after 30 min in presence of the blockers. *A*: addition of APV ( $50 \mu\text{M}$ ) plus CPP ( $50 \mu\text{M}$ ) to saline produces a small reduction in the size of an EPSP evoked by a single eighth nerve stimulus. *B*: same preparation and time points as in *A*, demonstrating that during repetitive stimulation of the eighth nerve there is a progressive build-up of the NMDA-mediated component. Second and third EPSP amplitudes are measured from the tail of the single pulse (as in Fig. 1).

2.5 mV from rest caused such a dramatic enhancement of the NMDA response.

In three of four experiments, there was a slight tendency for the slope of the  $I$ - $V$  curve to become less negative as the M cell was hyperpolarized by  $\sim 10$  mV beyond rest (Fig. 7B2 illustrates 1 example). However, the lack of stable clamp conditions at potentials far from resting potential prevented characterization of the voltage-dependence of the NMDA response  $> 10$  mV in either the de- or hyperpolarizing direction.

#### *Effect of repetitive stimulation on the amplitude of the APV-sensitive component*

Another characteristic of NMDA receptor-mediated transmission is its enhancement with repetitive firing (Herron et al. 1986). We have reported that induction of LTP of the eighth-nerve-evoked EPSP, using brief presynaptic tetanization, is similar to NMDA receptor-mediated LTP in hippocampus (Yang et al. 1990). We therefore asked if the APV-sensitive component might be enhanced during repetitive stimulation. For this purpose, we recorded single and multiple responses before and after superfusion with saline containing a mixture of two NMDA receptor blockers, APV ( $50 \mu\text{M}$ ) and CPP ( $50 \mu\text{M}$ ). As shown in Fig. 8, while the blockers only removed a small portion of the EPSP produced by a single stimulus in this case (Fig. 8A), their effects on the second and third EPSPs evoked at 2-ms intervals were progressively greater (Fig. 8B). In contrast, the successive EPSPs in the controls responses were facilitated (Fig. 8B), due in part to increased transmitter release (Lin and Faber 1988b). Thus the effects of APV and CPP indicate that the brief tetani we use to induce paired pulse-facilitation and even LTP appear to cause a dramatic NMDA receptor activation, significantly augmenting and prolonging the synaptic

response. The apparent shortening of the second and third coupling potentials in the presence of APV/ CPP (Fig. 8B) was not consistently observed.

#### *Effects of APV on a slow depression of eighth nerve responses*

We observed a striking effect of APV on a phenomenon heretofore not described in the M-cell system. This phenomenon was discovered when the paradigm that produces paired-pulse facilitation was repeated every 1–2 s: at steady state, the amplitude of the first chemical EPSP of the pair was smaller than that produced by a single stimulus at the same strength and frequency (Fig. 9). This depression develops over a period of  $\sim 20$  s when paired stimuli are given at 0.5 Hz (Fig. 9, *A* vs. *B*). In other words, there is a use-dependent depression of the EPSP that lasts for  $\geq 2$  s when the eighth nerve is stimulated repetitively at short intervals. It was not observed when the two stimuli were separated by intervals of  $\geq 10$  ms, and the electrotonic potential was not similarly affected. The requirement that paired stimuli be used to produce this depression suggests involvement of NMDA receptor activation.

Accordingly, when APV superfusion reduced the amplitude of a single EPSP, it also consistently diminished or abolished this long-lasting depression. In seven experiments, paired stimulation depressed the first EPSP before drug application by  $11.5 \pm 1.5\%$  relative to single stimulation, but after application, this depression was only  $7.7 \pm 1.7\%$  ( $n = 7$ ). Figure 10, *A1* and *A2* and *B1* and *B2*, are two examples of this APV effect. In the example of Fig. 10A, *1* and *2*, APV totally removed the use-dependent EPSP depression, as indicated by the supposition of steady state responses to single and double stimuli in Fig. 10A2. Furthermore, in two of these experiments, including that illustrated in Fig. 10A, washout of the drug caused partial recovery of the depression (not shown). The effects of ketamine or CPP on the depression were not tested. The possible role of NMDA receptor-coupled channels in this phenomenon will be considered in the DISCUSSION.

The results in Fig. 10B, *1* and *2*, also confirm the observation that NMDA-receptor activation contributes to the facilitation produced by repetitive stimulation, as the paired-pulse facilitation was decreased by APV. In experiments where facilitation was not complicated by a superimposed disynaptic inhibitory shunt, we found that it was significantly reduced, by  $6.5 \pm 2.7$  percentage points, from an average of  $18.3 \pm 3.8\%$ .

The presence of an inhibitory shunt after a fast EPSP might account for the absence of a dominant slow component typical of those generally associated with NMDA receptor-mediated EPSPs. Two lines of evidence argue against this interpretation of the data. First, when weak stimuli were used, it was possible to evoke excitation without significant inhibition. Second, the inhibition was blocked sometimes by superfusion with two inhibitory antagonists, picrotoxin and strychnine. Under these conditions, we can confirm the lack of inhibition by showing that there is no reduction in antidromic spike height after the test stimulus. Also, no inhibitory postsynaptic current was unmasked when the holding potential was displaced from the resting level during voltage-

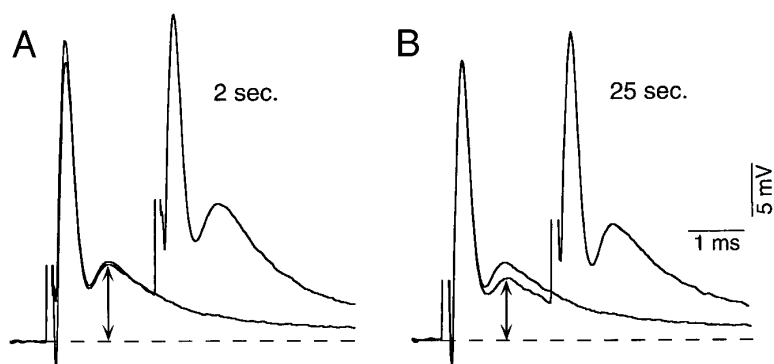


FIG. 9. Long-lasting depression after paired stimuli increases with time. A control trace, obtained by averaging the last 4 synaptic responses elicited by single stimuli (at 0.5 Hz), is compared with the average of the first 2 synaptic responses evoked by paired stimuli (*A*) and 2 obtained 25 s later (*B*). Whereas initially (2 s, *A*) the superimposed responses are comparable at steady state (25 s, *B*) the first chemical EPSP of the double response is smaller than that of the single (compare  $\leftrightarrow$  in *A* and *B*).

clamp experiments. Even after inhibition was blocked, there was no change in the EPSP time course or magnitude.

#### DISCUSSION

##### *Fast synaptic transmission at LMCE is mediated by two classes of glutamate receptors*

The experiments described here indicate that an excitatory amino acid, most likely glutamate, mediates chemical transmission at the eighth nerve synapses in the goldfish M cell. Interestingly, both, non-NMDA and NMDA receptors mediate fast synaptic transmission in this system. This conclusion arises from several independent lines of evidence, which include the use of specific pharmacological agonists and antagonists, the characterization of the voltage dependence of synaptic currents, and the consideration of previous functional (Pereda and Faber 1996; Yang et al. 1990) and immunohistochemical (Sur et al. 1994) studies, indicating the presence and physiological relevance of these glutamate receptor subtypes.

The fact that APV and ketamine removed a relatively late portion of the EPSP supports the hypothesis that this component arises from NMDA receptor activation. Nevertheless, the time course of the NMDA receptor-mediated component is unusually fast when compared with those ob-

served in other systems (Jahr 1994; McBain and Mayer 1994). That is, whereas NMDA synaptic currents are usually characterized by a long rise time ( $\approx 10$  ms) and slow decay time constant ( $>100$  ms), the APV-sensitive component of the synaptic response in the M cell is much faster, with a rise time of  $<1$  ms and decay time constant of only a few milliseconds. Although fast rise and decay times were reported for elementary NMDA-mediated synaptic currents in cerebellar granule cells (D'Angelo et al. 1990), the kinetics of the M-cell response are still quite unusual, particularly because our recordings were obtained at temperatures  $< 20^\circ\text{C}$ . In fact, the more important observation may be that the peak times of both the NMDA- and non-NMDA-mediated components in the M cell are quite fast and differ only slightly.

The experiments described here were performed *in vivo* and therefore with physiological concentrations of magnesium and glycine, an allosteric modulator of the NMDA receptor (Mayer et al. 1989), in the extracellular environment. Were it possible to remove magnesium under these experimental conditions, the drug-sensitive responses might have lasted much longer. This was found to be the case at the synapses between Rohan-Beard cells and dorsolateral spinal interneurons of *Xenopus* (Sillar and Roberts 1988), where removal of magnesium effectively increased the duration of the NMDA-mediated component from  $\sim 70$  to 220

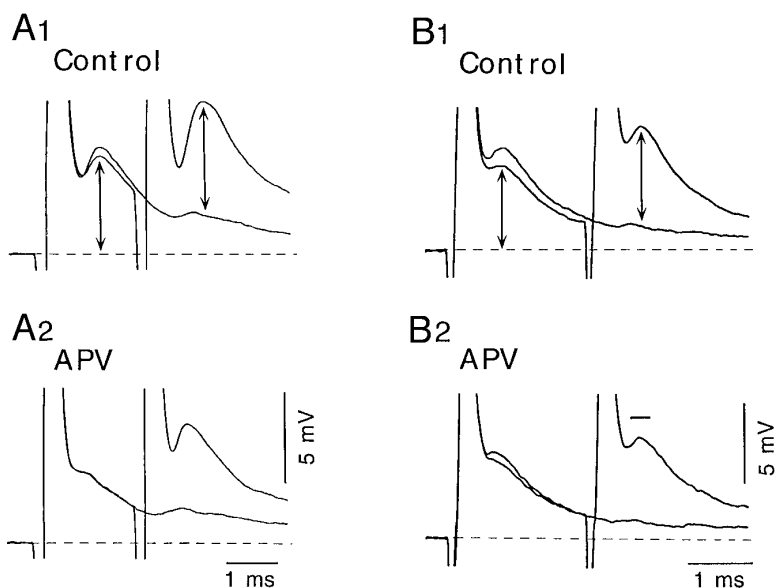


FIG. 10. APV removes a long-lasting depression of the first of 2 chemical EPSPs and reduces paired-pulse facilitation. *A1*: demonstration of the prolonged depression. Two superimposed traces (15 sweeps averaged in each) are shown, 1 from a single eighth nerve stimulus and 1 from a double. First chemical EPSP of the double is smaller than that of a single response. *A2*: in the presence of  $150 \mu\text{M}$  APV, the depression of the first EPSP is removed, so that the 2 EPSPs are completely superimposable. *B, 1* and *2*: APV-induced reduction of paired-pulse facilitation in another experiment. *B1*: amplitudes of the first and second EPSPs were measured as indicated ( $\leftrightarrow$ ), and the percent facilitation calculated as in the text. *B2*: both paired-pulse facilitation and long-lasting depression were reduced by  $20 \mu\text{M}$  APV. Bar over the second EPSP indicates the EPSP amplitude that would be required to achieve the same level of percent facilitation as in the control.

ms. Another possibility is that the NMDA receptor might be formed by an unusual combination of NMDA receptor subunits. Accordingly, it has been shown that on expression in cultured cells different heteromeric NMDA receptors channels differ in gating behavior and magnesium sensitivity (Monyer et al. 1992). It is conceivable then that a special combination of fish NMDA receptor subunit homologues could explain this unique behavior.

Nevertheless, the finding that NMDA receptors play a role in the production of such a rapid EPSP is novel and contrary to the generalization that fast potentials, such as those that participate in the generation of action potentials, are mediated by kainate or quisqualate receptors, whereas slower, modulatory potentials are mediated by NMDA receptors. Monosynaptic activation of NMDA and non-NMDA receptors by vestibular afferents has been reported for frogs (Boyle et al. 1991; Straka et al. 1996) and brain slices of the rat (Kinney et al. 1994; Takahashi et al. 1994). Interestingly, the rise-time of the NMDA receptor-mediated component in frogs was found to be significantly faster than that of other NMDA-mediated synaptic potentials in the same neurons, with the latter being comparable with NMDA receptor-mediated EPSPs of other systems (Straka and Dieringer 1996; Straka et al. 1996). Because NMDA receptor-mediated transmission in rat vestibular afferents was also fast (Kinney et al. 1994), it was suggested that NMDA receptors postsynaptic to vestibular afferents in both frogs and rats exhibit channels kinetics that are relatively fast (Straka et al. 1996).

#### *Voltage dependence and facilitation of synaptic responses*

Despite its fast kinetics this APV-sensitive component displays the voltage dependence (McBain and Mayer 1994) and enhancement with repetitive stimulation (Herron et al. 1986) that are characteristic features of NMDA receptor-mediated transmission (McBain and Mayer 1994). Responses to pressure-application of NMDA and glutamate were similarly voltage sensitive. The latter experiments are technically challenging, and it is difficult to rule out presynaptic actions of the agonists. Nevertheless, the limited series with glutamate and NMDA provided results consistent with the voltage dependence of the EPSC itself. In addition, it is unlikely that voltage-dependent currents intrinsic to the lateral dendrite contribute to this voltage dependence because none have been revealed in voltage-clamp studies of this neurite (Faber and Korn 1986).

We found that NMDA receptors augmented the chemical EPSP during brief bursts of repetitive firing, a presynaptic impulse pattern essential for induction of activity-dependent changes in synaptic strength (Pereda and Faber 1996; Yang et al. 1990). The receptors are involved even when only two stimulating pulses are used because low doses of APV produced a clear reduction in the amount of facilitation. This postsynaptic contribution to paired-pulse facilitation is indicated further by the observation that the larger the EPSP amplitude, the larger was the *relative* magnitude of the ketamine-sensitive component, presumably due to more channel unblocking with depolarization. Although the notion that NMDA receptors may play a role in paired-pulse facilitation at first seems to contradict those of Lin and Faber (1988b),

who concluded from quantal analysis that this facilitation arises from a presynaptic mechanism, one must bear in mind that those studies were performed using simultaneous recordings from single eighth nerve fibers and the M-cell dendrite. The EPSP produced by activating one of these fibers is small ( $0.139 \pm 0.075$  mV) and therefore is probably insufficient to trigger the voltage-dependent mechanism responsible for activation of NMDA receptors. It is thus likely that the degree of facilitation in the M cell produced by multiple stimuli is controlled by at least two distinct processes, one being presynaptic and the other postsynaptic. The latter would introduce a nonlinearity to the input-output relationship when a group of afferents are activated repetitively, for example by tone bursts (Fay and Olsho 1979; Furukawa and Ishii 1967). In addition, paired-pulse stimulation may lead to the transient build-up, at the receptors, of transmitter released by the same or adjacent terminals (Faber and Korn 1988).

#### *Use-dependent depression of EPSPs*

A second form of plasticity was observed with the paired-pulse paradigm. When steady state was reached during low-frequency stimulation, the first EPSP of a pair was always smaller than an EPSP produced by a single stimulus. This reduction was slow in onset and was reversible.

Interestingly, the depression of the EPSP was reduced by low doses of APV, suggesting a role for NMDA receptors in this phenomenon. One possible mechanism is that the NMDA receptors might undergo desensitization (Jahr 1994; Mayer and Westbrook 1987; Mayer et al. 1989; McBain and Mayer 1994; Tong et al. 1995). NMDA receptor-associated channels do show calcium-dependent desensitization, in that increases in intracellular calcium reduce their open probability in whole cell recordings, suggesting a possible feedback mechanism to control postsynaptic calcium levels (Legendre et al. 1993). Indeed, a phenomenon similar to the one reported here was described recently in hippocampal neurons in culture (Rosenmund et al. 1995), where synaptic NMDA receptors are inactivated by intracellular calcium, and calcium entry via synaptically activated NMDA receptors is sufficient to provide feedback inhibition of the NMDA-mediated component. Several mechanisms have been proposed to explain the action of calcium on NMDA receptors, including calcium-dependent enzymes such as calcineurin (Leiberman and Mody 1994; Tong et al. 1995). Modification of NMDA receptors also may underlie the gradually developing depression of the eighth nerve EPSP because it is only seen during repetitive stimulation, a firing pattern that optimizes NMDA receptor activation.

Repetitive presynaptic stimulation seems to produce both NMDA receptor-mediated facilitation and depression of the eighth nerve EPSP. Although the facilitation is almost instantaneous and short lasting, the moderate depression of the EPSP develops on a slower time scale and would be expected to reduce the potential for activity-dependent synaptic plasticity imparted by these receptors. For example, the threshold for inducing LTP might be lower during the initial phase of presynaptic tetanization than later.

### Functional significance of a NMDA receptor-mediated fast EPSP

The data presented here suggest that NMDA receptors at the synapses between auditory fibers and the M cell lateral dendrite function, as in other systems, to boost synaptic responses under certain physiological conditions. It is tempting to speculate that the unusual kinetics of the NMDA receptor-mediated EPSP is adapted to the high-frequency of auditory input signals to the M cell and to this neuron's unique cellular properties and functional role. M-cell activation triggers a startle response, which is crucial to the survival of the animal (Eaton and Hackett 1984; Zottoli 1977) but disadvantageous if it occurs too frequently. Consequently, the M-cell system has a set of physiological properties that prevents unnecessary firing yet ensures activation when sensory stimuli exceed a moderately high-threshold value (see Faber et al. 1989). These properties include a high M-cell resting potential, passive somato-dendritic membranes, and a low input resistance ( $\sim 200$  k $\Omega$ ) and a time constant ( $\approx 400$   $\mu$ s) that results in synaptic potentials having very short time constants of decay (1–2 ms). In contrast, there are some nonlinear properties of the dendrites that serve to enhance inputs of sufficient amplitude (Faber et al. 1989).

Our data indicate there is yet another nonlinear property of the M-cell membrane that boosts excitatory responses as the cell approaches threshold, namely, the participation of NMDA receptors in the synaptic response. These receptors render the eighth nerve excitatory responses extremely voltage sensitive, a property that also provides these synapses with a role in integrating depolarizing potentials from more than one source of sensory input. The terminations of the various sensory modalities on the M cell are segregated quite spatially from each other (see Faber and Korn 1978). For example, the visual input is localized to the ventral dendrite (Chang et al. 1987), whereas the saccular fiber and lateral line inputs are restricted to the distal (Faber et al. 1980; Furshpan 1964) and proximal parts of the lateral dendrite (Korn and Faber 1975b), respectively. However, none of these synapses are on dendritic spines, and thus are not electrically isolated from the others. It is therefore likely that a depolarization produced by one sensory input would have sufficient amplitude to enhance a nearly coincident PSP from another source, as long as one of them used voltage-sensitive NMDA receptors. Indeed, stimulation of the optic tectum produces EPSPs in the lateral dendrite that are of sufficient amplitude to activate these receptors (L. Wolszon, unpublished observations), even though the tectal input is on the ventral dendrite. As the behaving animal is likely to respond differently to a sound in isolation than to a sound paired with a visual image, it is conceivable that a NMDA receptor-like mechanism may operate to integrate more than one type of information. In presence of other stimuli, the NMDA receptor may act as a "coincidence detector" and its activation eventually may sensitize the M cell to auditory input, thereby reducing the behavioral threshold for sound-evoked escape responses. At the same time, the fast kinetics of the NMDA receptor-mediated EPSP preserve the short integration time of the M cell.

This work was supported in part by National Institute of Neurological Disorders and Stroke Grant NS-21848.

Present address of L. R. Wolszon: Dept. of Biological Sciences, Columbia University, New York, NY 10027.

Address for reprint requests: D. S. Faber, Dept. of Neurobiology and Anatomy, MCP ♦ Hahnemann School of Medicine, Allegheny University of the Health Sciences, 3200 Henry Ave., Philadelphia, PA 19129.

Received 7 March 1997; accepted in final form 2 July 1997.

### REFERENCES

- BARTELMEZ, G. W. Mauthner's cell and the nucleus motorius tegmenti. *J. Comp. Neurol.* 25: 87–128, 1915.
- BIRCH, P., GROSSMAN, C., AND HAYES, A. G. 6,7-Dinitro-quinoline-2,3-dione and 6-nitro,7-cyano-quinoline-2,3-dione antagonise responses to NMDA in the rat spinal cord via an action at the strychnine-insensitive glycine receptor. *Eur. J. Pharmacol.* 156: 177–180, 1988.
- BOYLE, Y., GOLDBERG, J. M., AND FABER, D. S. Vestibular-nerve inputs to vestibulospinal and vestibulo-ocular neurons of the squirrel monkey. In: *The Head-Neck Sensory-motor System*, edited by A. Berthoz, W. Graf and P. P. Vidal. New York: Wiley, 1991, p. 255–258.
- CHANG, Y., LIN, J.-W., AND FABER, D. S. Spinal inputs to the ventral dendrite of the teleost Mauthner cell. *Brain Res.* 417: 205–213, 1987.
- D'ANGELO, E., ROSSI, P., AND GARTHWAITE, J. Dual-component NMDA receptor currents at a single central synapse. *Nature* 346: 467–470, 1990.
- DAVIES, J., FRANCIS, A. A., JONES, A. W., AND WATKINS, J. C. 2-amino-phosphovalerate (2-APV), a potent and selective antagonist of amino acid-induced and synaptic excitation. *Neurosci. Lett.* 21: 77–81, 1981.
- DIAMOND, J. The activation and distribution of GABA and L-glutamate receptors on goldfish Mauthner neurones: an analysis of dendritic remote inhibition. *J. Physiol. (Lond.)* 158: 296–323, 1968.
- DIAMOND, J. AND ROPER, S. Analysis of Mauthner cell responses to iontophoretically delivered pulses of GABA, glycine and L-glutamate. *J. Physiol. (Lond.)* 232: 113–128, 1973.
- EATON, R. C. AND HACKETT, J. T. The role of the Mauthner cell in fast-starts involving escape in teleost fishes. In: *Neural Mechanisms of Startle Behavior*, edited by R. C. Eaton. New York: Plenum Press, 1984, p. 213–266.
- FABER, D. S., FETCHO, J. R., AND KORN, H. Neuronal networks underlying the escape response in goldfish. General implications for motor control. *Ann. NY Acad. Sci.* 563: 11–33, 1989.
- FABER, D. S., KAARS, C., AND ZOTTOLI, S. J. Dual transmission at morphologically mixed synapses: evidence from postsynaptic cobalt injections. *Neuroscience* 5: 433–440, 1980.
- FABER, D. S. AND KORN, H. Electrophysiology of the Mauthner cell: basic properties, synaptic mechanisms, and associated network. In: *Neurobiology of the Mauthner Cell*, edited by D. S. Faber and H. Korn. New York: Raven Press, 1978, p. 47–132.
- FABER, D. S. AND KORN, H. Instantaneous inward rectification in the Mauthner cell: a postsynaptic booster for excitatory inputs. *Neuroscience* 19: 1037–1043, 1986.
- FABER, D. S. AND KORN, H. Synergism at central synapses due to lateral diffusion of transmitter. *Proc. Natl. Acad. Sci. USA* 85: 8708–8712, 1988.
- FAY, R. R. AND OLSHO, L. W. Discharge patterns of lagenar and saccular neurons of goldfish eighth nerve: displacement sensitivity and directional characteristics. *Comp. Biochem. Physiol. A Physiol.* 62: 377–386, 1979.
- FUKAMI, Y., FURUKAWA, T., AND ASADA, Y. Excitability changes of the Mauthner cell during collateral inhibition. *J. Gen. Physiol.* 48: 581–600, 1964.
- FURSHPAN, E. J. Electrical transmission at an excitatory synapse in a vertebrate brain. *Science* 144: 878–880, 1964.
- FURSHPAN, E. J. AND FURUKAWA, T. Intracellular and extracellular responses of several regions of the Mauthner cell of the goldfish. *J. Neurophysiol.* 25: 732–771, 1962.
- FURUKAWA, T. AND ISHII, Y. Neurophysiological studies of hearing in goldfish. *J. Neurophysiol.* 30: 1377–1402, 1967.
- HABLITZ, J. J. AND SUTOR, B. Excitatory postsynaptic potentials in rat neocortical neurons in vitro. III. Effects of a quinoxalinedione non-NMDA receptor antagonists. *J. Neurophysiol.* 64: 1282–1290, 1990.
- HERRON, C. E., LESTER, R., COAN, E. J., AND COLLINDRIDGE, G. L. Frequency-dependent involvement of NMDA receptors in the hippocampus: a novel synaptic mechanism. *Nature* 309: 261–263, 1986.
- JAHR, C. NMDA receptor kinetics and synaptic function. *Semin. Neurosci.* 6: 81–86, 1994.

- JONES, A. W., SMITH, D.A.S., AND WATKINS, J. C. Structure-activity relations of dipeptide antagonists of excitatory amino acids. *Neuroscience* 13: 573–581, 1984.
- KINNEY, G. A., PETERSON, B. W., AND SLATER, N. T. The synaptic activation of *N*-methyl-D-aspartate receptors in rat medial vestibular nucleus. *J. Neurophysiol.* 72: 1588–1595, 1994.
- KORN, H. AND FABER, D. S. An electrically mediated inhibition in goldfish medulla. *J. Neurophysiol.* 38: 452–471, 1975a.
- KORN, H. AND FABER, D. S. Inputs from the posterior lateral line nerve upon the goldfish Mauthner cell. I. Properties and synaptic localization of the excitatory component. *Brain Res.* 95: 342–343, 1975b.
- LEGENDRE, P., ROSENKUND, C., AND WESTBROOK, G. L. Inactivation of NMDA channels in cultured hippocampal neurons by intracellular calcium. *J. Neurosci.* 13: 674–1312 1993.
- LIEBERMAN, D. N. AND MODY, I. Regulation of NMDA channel function by endogenous  $Ca^{++}$ -dependent phosphatase. *Nature* 369: 235–239 1994.
- LIN, J.-W. *Physiology and Morphology of Identified Mixed Excitatory Synapses on the Goldfish Mauthner Cell* (PhD thesis). Buffalo, NY: SUNY at Buffalo, 1986.
- LIN, J.-W. AND FABER, D. S. Synaptic transmission mediated by single club endings on the goldfish Mauthner cell. I. Characteristics of electrotonic and chemical postsynaptic potentials. *J. Neurosci.* 8: 1302–1312 1988a.
- LIN, J.-W. AND FABER, D. S. Synaptic transmission mediated by single club endings on the goldfish Mauthner cell. II. Plasticity of excitatory postsynaptic potentials. *J. Neurosci.* 8: 1313–1325 1988b.
- LIN, J.-W., FABER, D. S., AND WOOD, M. R. Organized projection of the goldfish saccular nerve onto the Mauthner cell lateral dendrite. *Brain Res.* 274: 319–324 1983.
- MACDONALD, J. F., MILKOVIC, Z., AND PENNEFATHER, P. Use-dependent block of excitatory amino acid currents in cultured neurons by ketamine. *J. Neurophysiol.* 58: 251–266 1987.
- MALENKA, R. C. AND NICOLL, R. A. NMDA-receptor-dependent synaptic plasticity: multiple forms and mechanisms. *Trends Neurosci.* 16: 521–527 1993.
- MAYER, M. L., VYKLYCKY, L., JR., AND CLEMENTS, J. Regulation of NMDA receptor desensitization in mouse hippocampal neurons by glycine. *Nature* 338: 425–427 1989.
- MAYER, M. L. AND WESTBROOK, G. L. Mixed-agonist action of excitatory amino acids on mouse spinal cord neurons under voltage-clamp. *J. Physiol. (Lond.)* 354: 29–53 1984.
- MAYER, M. L. AND WESTBROOK, G. L. The physiology of excitatory amino acids in the vertebrate CNS. *Prog. Neurobiol.* 28: 197–276 1987.
- MAYER, M. L., WESTBROOK, G. L., AND GUTHRIE, P. B. Voltage-dependent block by  $Mg^{2+}$  of NMDA responses in spinal cord neurons. *Nature* 309: 261–263 1984.
- MCBAIN, C. J. AND MAYER, L. *N*-methyl-D-aspartic receptor structure and function. *Physiol. Rev.* 74: 723–760 1994.
- MONYER, H., SPRENGEL, R., SCHOEPE, R., HERB, A., HIGUCHI, M., LOMELLI, H., BURNASHEV, N., SAKMANN, B., AND SEEBURG, P. Heteromeric NMDA receptors: molecular and functional distinction of subtypes. *Science* 256: 1217–1221 1992.
- NAKAJIMA, Y. AND KOHNO, K. Fine structure of the Mauthner cell: synaptic topography and comparative study. In: *Neurobiology of the Mauthner Cell*, edited by D. S. Faber and H. Korn. New York: Raven Press, 1978, p. 133–166.
- NOWAK, L., BREGESTOVSKI, P., ASCHER, P., HERBET, A., AND PROCHIANTZ, A. Magnesium gates glutamate-activated channels in mouse central neurons. *Nature* 307: 462–465 1984.
- PEREDA, A. AND FABER, D. S. Activity-dependent short-term enhancement of intercellular coupling. *J. Neurosci.* 16: 983–992 1996.
- PEREDA, A., NAIRN, A., WOLSZON, L., AND FABER, D. S. Postsynaptic modulation of synaptic efficacy at mixed synapses on the Mauthner cell. *J. Neurosci.* 14: 3704–3712 1994.
- PEREDA, A., TRILLER, A., KORN, H., AND FABER, D. S. Dopamine enhances both electrotonic coupling and chemical excitatory postsynaptic potentials at mixed synapses. *Proc. Natl. Acad. Sci. USA* 89: 1208–1209 1992.
- ROSENKUND, C., FELTS, A., AND WESTBROOK, G. L. Calcium-dependent inactivation of synaptic NMDA receptors in hippocampal neurons. *J. Neurophysiol.* 73: 427–430 1995.
- SILLAR, K. T. AND ROBERTS, A. Unmyelinated cutaneous afferent neurons activate two types of excitatory amino acid receptor in the spinal cord of *Xenopus laevis* embryos. *J. Neurosci.* 8: 1350–1360 1988.
- SILVA, A., KUMAR, S., PEREDA, A., AND FABER, D. S. Regulation of synaptic strength at mixed synapses: effects of dopamine receptor blockade and protein kinase C activation. *Neuropharmacology* 34: 1559–1565 1995.
- STONE, T. W. AND BURTON, N. R. NMDA receptors and ligands in the vertebrate CNS. *Prog. Neurobiol.* 30: 333–368 1988.
- STRAKA, H., DEBLER, K., AND DIERINGER, N. Size-related properties of vestibular afferent fibers in the frog: differential synaptic activation of *N*-methyl-D-aspartate and non-*N*-methyl-D-aspartate receptors. *Neuroscience* 70: 697–707 1996.
- STRAKA, H. AND DIERINGER, N. Uncrossed disynaptic inhibition of second-order vestibular neurons and its interaction with monosynaptic excitation from vestibular nerve afferent fibers in the frog. *J. Neurophysiol.* 76: 3087–3101 1996.
- SUR, C., WENTHOLD, R., AND TRILLER, A. Differential cellular distribution of excitatory amino acid receptor sub-units on the M-cell of teleost. *Soc. Neurosci. Abstr.* 20: 489, 1994.
- TAKAHASHI, Y., TSUMOTO, T., AND KUBO, T. *N*-methyl-D-aspartate receptors contribute to afferent synaptic transmission in the medial vestibular nucleus of young rats. *Brain Res.* 659:287–291 1994.
- THOMSON, A. M. AND RADPOUR, S. Local circuit connections mediated by NMDA and non-NMDA receptors in slices of neocortex. *Adv. Exp. Med. Biol.* 268: 313–21 1990.
- TITMUS, M., KORN, H., AND FABER, D. S. Diffusion, not uptake, limits glycine concentration in the synaptic cleft. *J. Neurophysiol.* 75: 1738–1752 1996.
- TONG, G., SHEPHERD, D., AND JAHR, C. E. Synaptic desensitization of NMDA receptors by calcineurin. *Science* 267: 1510–1512 1995.
- TUTTLE, R., MASUKO, S., AND NAKAJIMA, Y. Freeze fracture study of the large myelinated club ending synapse on the goldfish Mauthner cell: special reference to the quantitative analysis of gap junctions. *J. Comp. Neurol.* 246, 202–211 1986.
- WOLSZON, L. AND FABER, D. S. Fast EPSPs evoked in the Mauthner cell by sensory afferents are due to NMDA receptor activation. *Soc. Neurosci. Abstr.* 14: 939, 1988.
- YAMADA, K., DUBINSKY, J. M., AND ROTHMAN, S. M. Quantitative physiological characterization of a Quinoxalinedione non-NMDA receptor antagonist. *J. Neurosci.* 9: 3230–3236 1989.
- YANG, X. D., FABER, D. S. Initial synaptic efficacy influences induction and expression of long-term changes in transmission. *Proc. Natl. Acad. Sci. USA* 88: 4299–4303 1991.
- YANG, X. D., KORN, H., AND FABER, D. S. Long-term potentiation of electrotonic coupling at mixed synapses. *Nature* 348: 542–545 1990.
- ZOTTOLI, S. J. Correlation of the startle reflex and Mauthner cell auditory responses in unrestrained goldfish. *J. Exp. Biol.* 66: 243–254 1977.